Tetrahedron 65 (2009) 2399–2407

Contents lists available at ScienceDirect

Tetrahedron

journal homepage: www.elsevier.com/locate/tet

Amphiphilic dipyrrinones: methoxylated [6]-semirubins

Sanjeev K. Dey, David A. Lightner *

Department of Chemistry, University of Nevada, Reno, NV 89557-0216, USA

ARTICLE INFO

Article history:
Received 4 November 2008
Received in revised form 11 December 2008
Accepted 6 January 2009
Available online 14 January 2009

Keywords:
Dipyrroles
NMR
X-ray crystallography
Aqueous solubility

ABSTRACT

Replacing the typical β-alkyl substituents of [6]-semirubin and [6]-oxosemirubin, two intramolecularly hydrogen-bonded bilirubin analogs, with methoxy groups produces amphiphilic dipyrrinones. Synthesized from the respective 9*H*-dipyrrinones prepared by base-catalyzed condensation of 3,4-dimethoxypyrrolin-2-one with the appropriate pyrrole α-aldehyde, the 2,3-dimethoxy and 2,3,7,8-tetramethoxy analogs of [6]-semirubin are yellow-colored dipyrrinones that form intramolecularly hydrogen-bonded monomers in $CDCl_3$, as deduced from ^1H NMR NH chemical shifts. They are monomeric in $CHCl_3$, as determined by vapor pressure osmometry. In contrast, in the solid, X-ray crystallography reveals supramolecular ribbons of intermolecularly hydrogen-bonded (dipyrrinone to dipyrrinone and acid to acid) 2,3,7,8-tetramethoxy-[6]-semirubin. The latter is approximately 20 times more soluble in water than the parent [6]-semirubin with four β-methyl groups.

1. Introduction

Bilirubin (Fig. 1A), the yellow pigment of jaundice and the end product of heme metabolism,[1] is very insoluble in water (K_{sp} $\sim 4\times10^{-15}$ M at pH 7 at 37 °C),[2] which makes it unexcretable except by formation of glucuronide conjugates, the main pathway for its elimination. The pigment's poor aqueous solubility is explained by a ridge-tile conformation,[3–5] wherein the propionic acids are tucked inward and firmly hydrogen bonded to the opposing dipyrrinones, thereby presenting a hydrocarbon-like periphery (Fig. 1B). Insightful studies of bilirubin chemistry, photobiology, and metabolism have been advanced from its dipyrrinone[6] models, inter alia. Among such analogs of bilirubin, [6]-semirubin (Fig. 1C)[7] was synthesized in order to evaluate carboxylic acid to amide hydrogen bonding. [6]-Semirubin, like bilirubin, is lipophilic and insoluble in water. Interest in improving the aqueous solubility of bilirubin and thereby facilitating its elimination led us to synthesize a bilirubin with an MW 2200 polyethylene glycol unit attached at the *exo*-vinyl group. The bilirubin derivative was soluble in both water and $CHCl_3$ but was present as an aggregate in water (presumably with bilirubin molecules aggregated inside a polyether micelle).[8] Shorter, single polyethylene glycol chains led to decreased aqueous solubility. To prepare a water-soluble pigment that was not aggregated, we considered the possibility that multiple, short polyethylene glycol units might produce the desired aqueous solubility without aggregation. Merz et al.,[9a] and Sessler et al.,[9b] and Schmuck and Wienand[9c] counteracted the intrinsic aqueous insolubility of porphyrins and pyrroles by attaching short polyether chains, e.g., diethylene glycol, at the pyrrole β-positions, which suggested that replacing some of the pyrrole β-substituents of bilirubin might produce a similar salutary effect by improving the pigment's aqueous solubility and avoiding aggregation. While considering the feasibility of synthesizing bilirubinoids and model dipyrrinones with di- or triethylene glycol β-substituents, we decided to explore whether even the smallest β-ether (OCH_3) substituent might improve the aqueous solubility of the pigment. In the current study we focused on the model for one-half of bilirubin, the dipyrrinone [6]-semirubin, in order to learn to what extent replacing its lactam and pyrrole β-substituents with methoxy groups might (1) enhance the pigment's aqueous solubility and (2) avoid aggregation in water. In the following we describe the syntheses, solution structures, and solubilities of tetramethoxy (**1**) and dimethoxy (**2**) analogs (Fig. 1D) of [6]-semirubin. We also report the syntheses of the corresponding 9^1-oxo analogs (**3** and **4**) and compare their properties to [6]-oxosemirubin (Fig. 1C). X-ray crystallographic structures of **1** and the ethyl ester (**4e**) of **4** were obtained.

2. Results and discussion

2.1. Synthesis

The key intermediates for the synthesis of methoxylated [6]-semirubins (**1**–**4**) are 9*H*-dipyrrinones: tetramethoxy **5** and dimethoxy **6**, which were available from earlier work.[10] Reaction of the latter under Friedel–Crafts acylation conditions using the half ester acid chloride of adipic acid afforded [6]-oxosemirubin analogs **3e**

* Corresponding author. Tel.: +1 775 784 4980; fax: +1 775 784 6804.
E-mail address: lightner@scs.unr.edu (D.A. Lightner).

0040-4020/$ – see front matter © 2009 Elsevier Ltd. All rights reserved.
doi:10.1016/j.tet.2009.01.028

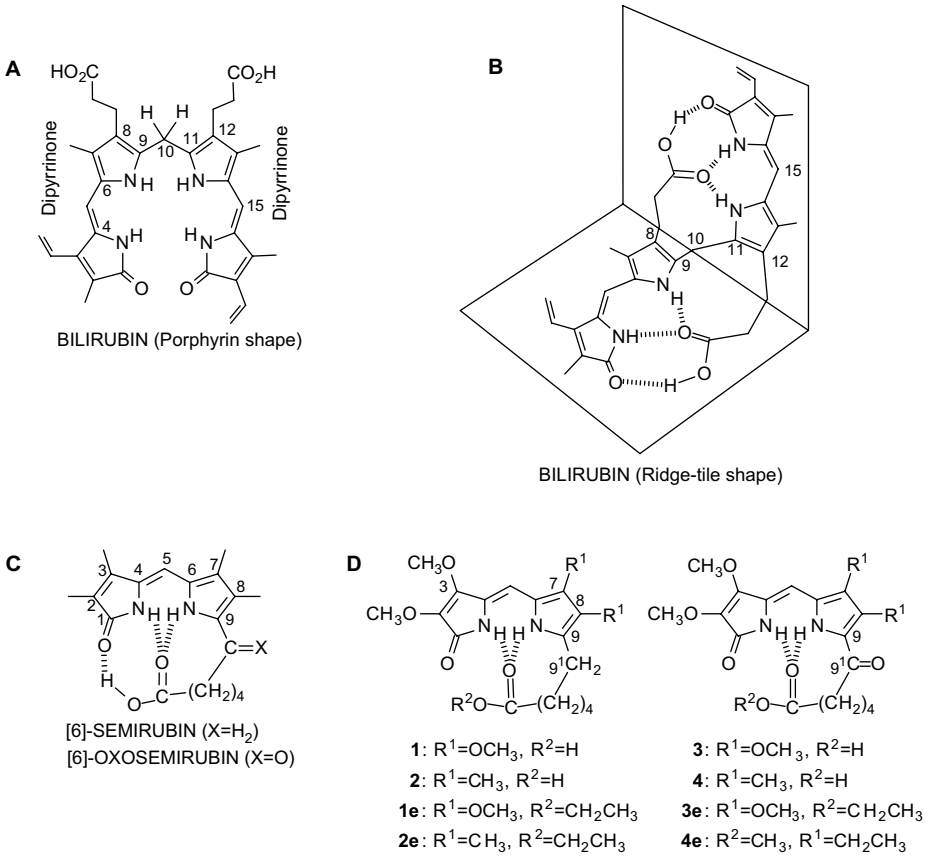

Figure 1. (A) Porphyrin-like representation of bilirubin. (B) The most stable conformation of bilirubin is neither porphyrin-like nor linear but shaped like a ridge-tile and stabilized by intramolecular hydrogen bonding. (C) The semirubin model for one-half of intramolecularly hydrogen-bonded bilirubin and its oxo analog. (D) The target methoxy [6]-semirubins of this work.

and **4e**, from **5** and **6**, respectively. The esters were saponified to the corresponding acids (**3** and **4**). Reduction of **3e** and **4e** using $NaBH_4$+boron trifluoride etherate afforded the corresponding ethyl esters **1e** and **2e**. Reduction of **3e** and **4e** using $NaBH_4$ in 2-propanol followed by saponification in the same reaction pot gave semirubin analogs **1** and **2** (Scheme 1).

2.2. Structures and NMR spectroscopy

The constitutional structures of **1**–**4** and **1e**–**4e** follow from the 9*H*-dipyrrinone precursors **5** and **6** and comparison of their ^{13}C NMR spectral data (Table 1) with those of the parent [6]-semirubin and [6]-oxosemirubin and their esters.[6] The methoxy carbons at

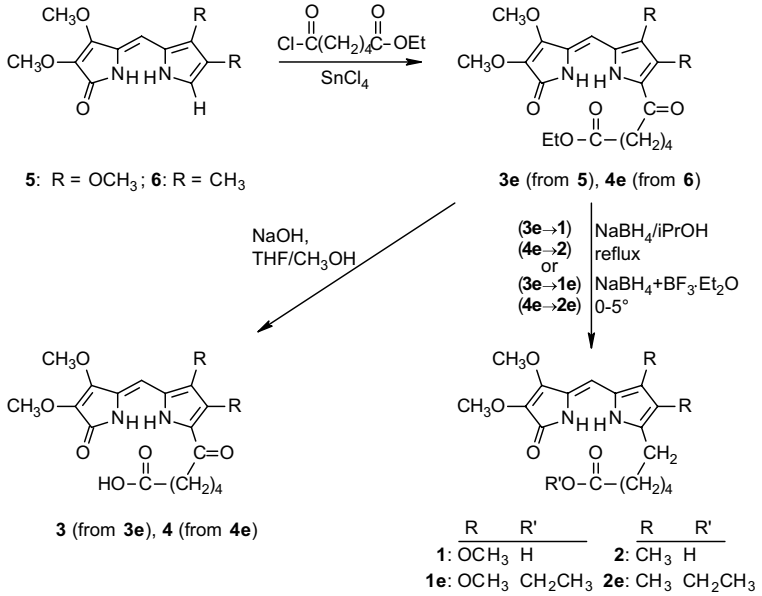

Scheme 1.

Table 1
Comparison of the ^{13}C NMR chemical shifts (δ, ppm)[a] of semirubins **1** and **2**, oxosemirubins **3** and **4**, and their ethyl esters **1e**–**4e**

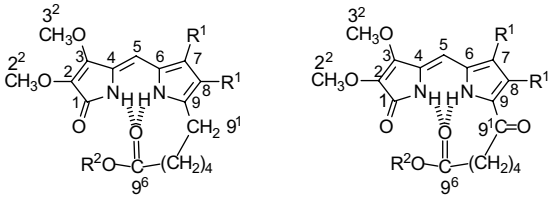

	R^1	R^2	
1	OCH_3	H	**3**
2	CH_3	H	**4**
1e	OCH_3	CH_2CH_3	**3e**
2e	CH_3	CH_2CH_3	**4e**

		1	**1e**	**2**	**2e**	**3**	**3e**	**4**	**4e**
1	C=O	169.2	166.6	169.3	168.5	166.2	165.9	170.1	168.6
2	=C–	126.80	127.1	126.5	126.3	128.2	128.2	127.7	127.7
3	=C–	148.4	147.1	148.5	149.1	145.4	145.3	147.5	147.0
4	=C–	119.7	122.0	122.4	122.1	130.3	130.4	126.6	126.7
5	=CH	99.0	98.4	100.9	101.1	95.4	95.4	98.1	96.8
6	=C–	112.8	112.4	119.6	118.9	123.4	123.2	128.3	127.9
7	=C–	141.6	140.9	125.7	125.8	135.6	135.41	125.2	124.3
8	=C–	135.7	136.2	116.3	116.1	144.3	144.1	128.0	129.1
9	=C–	126.9	124.3	135.9	136.3	119.2	119.1	131.0	131.3
9^1	CH_2 or C=O	22.0	24.6	23.4	29.9	189.6	189.5	190.9	190.4
9^2	CH_2	28.8	29.0	28.6	28.8	38.9	38.9	39.9	39.9
9^3	CH_2	26.7	28.5	26.7	26.6	24.7	24.9	24.8	24.9
9^4	CH_2	21.6	24.3	21.9	25.0	24.4	24.4	24.0	24.1
9^5	CH_2	33.1	34.3	33.3	34.5	33.9	34.3	33.6	34.4
9^6	C=O	181.0	174.3	180.9	174.1	178.4	173.8	179.8	173.8
9^8	CH_2	—	60.6	—	60.4	—	62.8	—	61.1
9^9	CH_3	—	14.4	—	14.5	—	14.4	—	14.4
2^2	OCH_3	61.3	61.4	61.3	61.7	60.9	61.0	61.0	60.5
3^2	OCH_3	59.5	59.4	59.4	59.3	59.6	59.6	59.5	59.5
7^1	CH_3	—	—	9.8	9.9	—	—	11.5	11.9
8^1	CH_3	—	—	9.0	9.3	—	—	9.3	9.5
7^2	OCH_3	62.4	62.2	—	—	62.8	62.9	—	—
8^2	OCH_3	61.8	61.8	—	—	60.9	60.5	—	—

[a] Measured in $CDCl_3$ at 23 °C for 5×10^{-3} M concentration.

C(2) and C(3) appear in the expected ranges, with the *endo* OCH_3 (at C(3)) more shielded than the *exo* (at C(2)); however, C(4) of **1** and **2** is shifted 4–8 ppm upfield relative to **3** and **4**. The latter show signals near 190 ppm for the 9^1-oxo group. The presence of the semirubin acids is evident by the deshielding of the CO_2H carbon (~180 ppm) compared to that of the esters (~174 ppm).

2.3. Solution molecularity

Using vapor pressure osmometry (VPO) to determine molecular weights in solution, all of the acids (**1**–**4**) were shown to be monomers in both $CHCl_3$ (Table 2). The data are consistent with intramolecularly hydrogen-bonded species, found in the parent [6]-semirubin and [6]-oxosemirubin.[7] As expected from earlier studies of dipyrrinones,[6,7,11] esters **1e** and **2e** were dimeric in $CHCl_3$, but oxosemirubin esters **3e** and **4e** were monomeric. The latter is attributed to the oxo group being oriented in such a way that the ester chain blocks formation of intermolecular hydrogen bonding between the dipyrrinones.[11]

2.4. Intramolecular hydrogen bonding from ^1H NMR spectroscopy

Intramolecular hydrogen bonding in [6]-semirubin (Fig. 1C) in $CDCl_3$ was firmly established previously[7] by ^1H NMR and Nuclear Overhauser Effect (NOE) measurements. NOEs in $CDCl_3$ in **1**–**4** found between the lactam and pyrrole NHs (Fig. 2), and between the C(5)–H and the neighboring OCH_3/CH_3 groups confirm the *syn-Z* configuration of the dipyrrinone. Weak NOEs between the

Table 2
Molecular weight (MW) of semirubins **1** and **2** and their ethyl esters (**1e** and **2e**) and oxosemirubins **3** and **4** and their ethyl esters (**3e** and **4e**) determined by vapor pressure osmometry[a] at 45 °C in $CHCl_3$ solution[b]

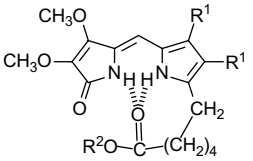

1, 2, 1e, 2e

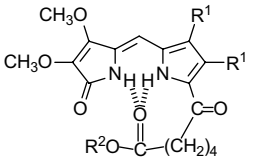

3, 4, 3e, 4e

	R^1	R^2	Formula weight (FW, g mol^{-1})	Measured MW (g mol^{-1})
1	OCH_3	H	394	351±28
2	CH_3	H	362	351±27
3	OCH_3	H	408	450±27
4	CH_3	H	376	392±20
1e	OCH_3	CH_2CH_3	422	865±31
2e	CH_3	CH_2CH_3	390	798±15
3e	OCH_3	CH_2CH_3	436	471±33
4e	CH_3	CH_2CH_3	404	433±17

[a] Calibrated with benzil (FW=210 g mol^{-1}, MW=220±15 g mol^{-1}).
[b] Concn. range $0.5–2.0\times10^{-3}$ mol kg^{-1}.

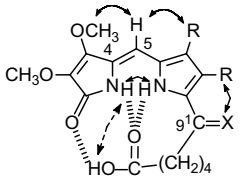

1: R = OCH_3 **2**: R = CH_3 X=H_2
3: R = OCH_3 **4**: R = CH_3 X=O

Figure 2. Nuclear Overhauser Effect (NOE) correlations (shown by double-headed arrows) found in $CDCl_3$ for **1** and **2** (X=H_2) and **3** and **4** (X=O). In the latter, the correlation at 9^1 is absent because there are no hydrogens at C(9^1) in **3** and **4**. Weak correlations are indicated by dashed double-headed arrows.

CO_2H and the lactam NH confirm intramolecular hydrogen bonding. In addition, **1** and **2** exhibit deshielded NH chemical shifts commensurate with hydrogen bonding to the hexanoic acid carbonyl (Table 3) and not much different from those found in [6]-semirubin.[7] The OCH_3 groups cause small upfield shifts of the NH signals. As in [6]-semirubin the relevant NOEs support the intramolecularly hydrogen-bonded 4*Z*-configuration structure. Similarly, at least some intramolecular hydrogen bonding is detected in the [6]-oxosemirubin analogs **3** and **4**, as has been seen in [6]-oxosemirubin itself.[7]

2.5. X-ray crystal structures of 1 and 4e

Despite the large number of known dipyrrinones, only a few X-ray crystal structures of them have been obtained.[6,10a,12] They all have the common feature of in-plane dipyrrinone to dipyrrinone hydrogen bonding. Until the present work there have been no crystal structures published of a semirubin, despite earlier attempts. Figures 3 and 4 present the crystal structure drawings from crystals of **1** and **4e** grown from diethyl ether–1,2-dichloroethane and $CHCl_3$–*n*-hexane, respectively. The constitutional structures of **1** and **4e** are fully confirmed in their crystal structures. In the unit cells, there are two distinct (A and B) molecules of **1** (Fig. 3A) but for **4e** there is one molecule (Fig. 4A).

Table 3
Comparison of the ^{1}H NMR chemical shifts (δ, ppm) of the lactam and pyrrole NH and carboxylic acid OH of semirubins **1** and **2** and their ethyl esters (**1e** and **2e**), oxosemirubins **3** and **4** and their ethyl esters (**3e** and **4e**), and [6]-semirubin and [6]-oxosemirubin[a]

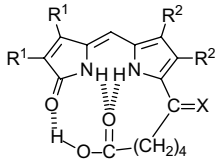

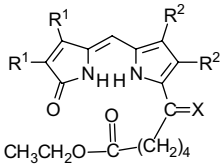

Dipyrrinone	R^1	R^2	X	Lactam/NH	Pyrrole/NH	CO_2H
1	OCH_3	OCH_3	H_2	10.11	8.38	12.74
2	OCH_3	CH_3	H_2	10.07	8.80	13.20
Semirubin	CH_3	CH_3	H_2	10.48	8.98	13.22
3	OCH_3	OCH_3	O	9.12	8.53	11.95
4	OCH_3	CH_3	O	9.10	10.15	11.93
Oxo semi	CH_3	CH_3	O	9.21	10.66	12.80
1e	OCH_3	OCH_3	H_2	9.13	8.13	—
2e	OCH_3	CH_3	H_2	10.37	9.66	—
Semi ester	CH_3	CH_3	H_2	11.17	10.11	—
3e	OCH_3	OCH_3	O	9.55	8.53	—
4e	OCH_3	CH_3	O	8.14	9.27	—
Oxo ester	CH_3	CH_3	O	8.05	9.14	—

[a] Measured in $CDCl_3$ at 23 °C for 1×10^{-3} M solutions.

Based on all previous and current studies of [6]-semirubin, we had fully expected an intramolecularly hydrogen-bonded structure for **1**. Yet in the crystal it is found to be *inter*molecularly hydrogen bonded, dipyrrinone to dipyrrinone and carboxylic acid to carboxylic acid, to form stacked, parallel streams of supramolecular ribbons (Fig. 3B) with the parallel stacks of ribbons separated by 7.8 Å. The dipyrrinones are nearly planar, with relevant torsion angles, N(1)–C(4)=C(5)–C(6)=3.3° in A and 0.3° in B, and C(4)=C(5)–C(6)–C(6)–N(2)=4.2° in A and 0.9° in B, which confirm a planar *syn-Z* configuration. All dipyrrinone bond lengths and bond angles of **1** (Fig. 5A) conform to those measured in previous crystal structures[10a,12] and can thus be viewed as 'normal,' with alternating double and single bonds.

In contrast to **1**, the oxosemirubin ester (**4e**) was not expected to be intramolecularly hydrogen bonded. In the crystal, **4e** is intermolecularly hydrogen bonded, dipyrrinone to dipyrrinone; however, the dipyrrinone units of the hydrogen-bonded pair do not lie co-planar but are orthogonal (Fig. 4B). The dipyrrinones of **4e** are only slightly less planar than in **1**, as indicated by the relevant torsion angles: N(1)–C(4)=C(5)–C(6)=4.9° and C(4)=C(5)–C(6)–N(2)=8°. The dipyrrinone conformation is thus again shown to be *syn-Z*, and the 9^1-oxo group is found to be *syn* to the pyrrole nitrogen. The presence of the 9^1-oxo induces some interesting changes in the dipyrrinone bond angles and bond lengths (Fig. 5B) relative to those of **1**. Thus, while the alternating double and single bonds of the pyrrole ring of **1** (Fig. 5A) are blurred into a single value near 1.4 Å, they remain distinct in the lactam ring, with somewhat (0.15–0.20 Å) lengthened N(1)–C(1), C(1)–C(2), and C(3)–C(4) bond lengths in **4e** relative to **1**. Similarly, C(5)–C(6) is lengthened by 0.15 Å in **4e** relative to **1**, but the C(2)=C(5) and C(4)=C(5) double bond lengths remain essentially unchanged. The significant changes in bond angles indicate a widening of the N(1)–C(4)=C(5)–C(6)–N(2) cavity of **4e** relative to **1**, possibly to accommodate the orthogonal hydrogen bonding motif in the former. Again, other differences in bond angles lie mainly in the pyrrole ring.

2.6. Solubility

The characterization of methoxylated-dipyrrinones **1**–**4** indicates great similarity in solution structure and hydrogen bonding to the parent [6]-semirubin and [6]-oxosemirubin parents. The acids (**1**–**4**) and their esters (**1e**–**4e**) are more soluble in $CHCl_3$ and in CH_3OH than the parents. In H_2O, where the parent (tetramethyl) semirubins are very insoluble, the methoxylated analogs show better solubility. (Comparison of **1** and **1e** to **2** and **2e**, as well as **3** and **3e** to **4** and **4e** is shown in Table 4.) Thus, we examined their aqueous solubility as well as their solubility in CH_3OH (as a control). UV–vis spectroscopy was used to determine the concentrations relative to standard $\sim1\times10^{-5}$ M solutions. The CH_3OH control experiment shows that the solubility of the pigment at $1–3\times10^{-5}$ M in pure CH_3OH is almost exactly as that in CH_3OH–2% $CHCl_3$ (vol/vol) in which the pigment is freely soluble. All of the pigments are also freely soluble in a reference standard: H_2O–2% $(CH_3)_2SO$ (vol/vol). Comparing pure H_2O to this reference (Table 4), one finds that **1** is approximately 10 times more soluble in water than **2** and that while **1** is ~30% more soluble than its ester, **1e**, and **1e** is 15 times more soluble than **2e** at saturation.

The data reveal, as expected, that the presence of four methoxyl groups improves the aqueous solubility more than the two methoxyl groups of **2**, but that while the presence of a 9^1-oxo group does not improve the solubility (of **3**) relative to **1**, the 9^1-oxo groups in **4** and **4e** have a major effect on improving (4–6 times) the aqueous solubility of **2** and **2e**.

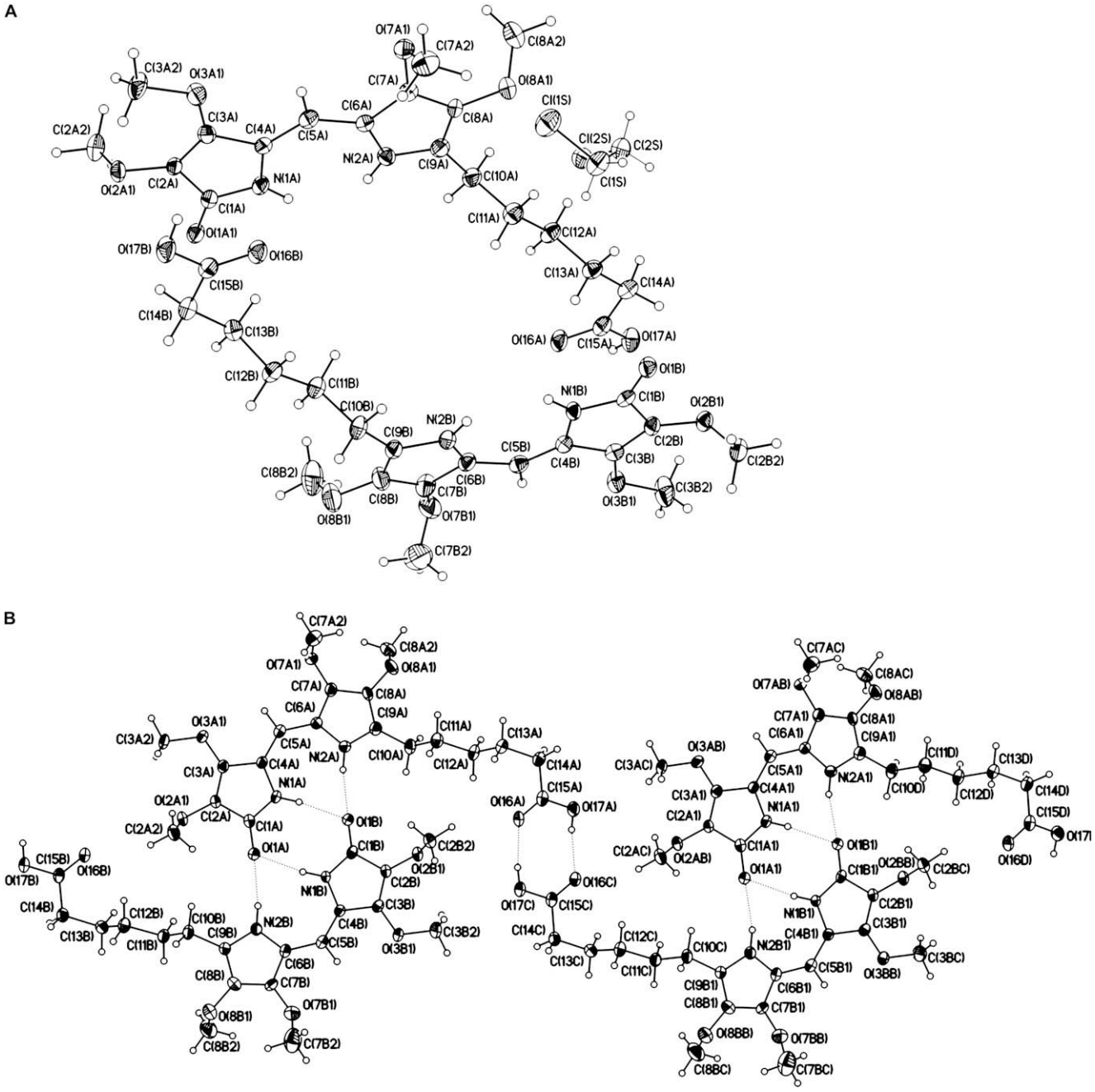

Figure 3. Crystal structure drawings of **1**: (A) the **A** and **B** molecules in the unit cell and their numbering system; (B) the intermolecularly hydrogen-bonded **A** and **B** molecules in supramolecular ribbons that are stacked in the third dimension (not shown).

2.7. UV–vis spectral data

UV–vis spectroscopy of **1**–**4** (Table 5) reveals several interesting facts. In general, the long wavelength dipyrrinone absorption of the tetramethoxy analogs (**1** and **3**) is shifted 5–6 nm hypsochromic relative to the dimethoxy analogs (**2** and **4**). This trend generally carries over to their esters, **1e** and **3e** versus **2e** and **4e**. The oxosemirubin long wavelength absorption is generally centered at a shorter λ_{max} than the corresponding semirubin analogs. Chloroform solutions, of **1**–**4**, in which the semirubins are intramolecularly hydrogen bonded produce bathochromically shifted long wavelength absorptions relative to CH_3OH, $(CH_3)_2SO$, and H_2O solutions, and the λ_{max} and ε_{max} in the latter three solvents are nearly the same. In contrast, esters **1e** and **2e** exhibit somewhat shorter wavelength λ_{max} in $CHCl_3$ relative to CH_3OH, $(CH_3)_2SO$, and H_2O solvents, while the reverse is found for the oxosemirubin esters **3e** and **4e**.

3. Concluding comments

The presence of methoxyl groups on the lactam and pyrrole β-positions of [6]-semirubin and [6]-oxosemirubin (to give **1**, **2** and **3**, **4**, Fig. 1C) improves their water solubility, with four methoxyl groups (of **1**) providing up to 0.06 M solutions (**1** and **3**) and up to 0.04 M solutions of the corresponding ethyl esters. However, the aqueous solubility was insufficient to analyze for aggregation by VPO. Nonetheless, the studies indicate that with di-, tri- or tetraethylene glycol chains, the semirubins should be sufficiently water soluble for analysis by VPO. The acids (**1**–**4**) form intramolecularly hydrogen-bonded monomers in $CHCl_3$ solvent whereas the

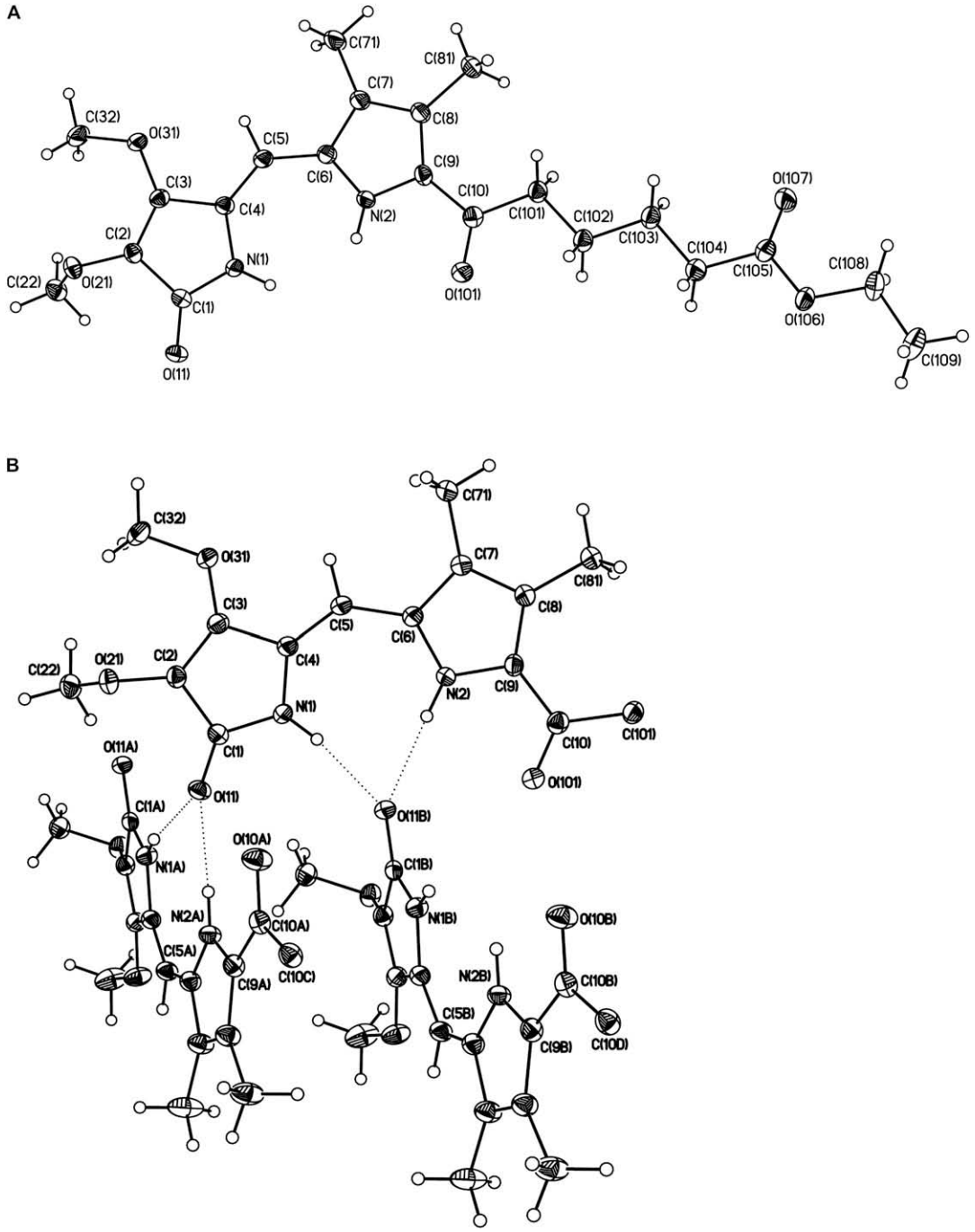

Figure 4. (A) Crystal structure drawing of dimethoxy-[6]-oxosemirubin ethyl ester (**4e**) with numbering system used. (B) Intermolecularly hydrogen bonding organization pattern of molecules of **4e** in the crystal, showing orthogonally positioned dipyrrinones. The carboxyethylpentanoyl side chains are truncated between carbons 9^2 and 9^3 for clarity of representation.

[6]-semirubin esters **1e** and **2e** are intermolcularly hydrogen-bonded dimers. In contrast, in the crystal, **1** is intermolecularly hydrogen bonded in supramolecular ribbons.

4. Experimental section

4.1. General procedures

All nuclear magnetic resonance (NMR) spectra were obtained on a Varian 500 MHz (^{1}H) and 125 MHz (^{13}C) in deuteriochloroform unless otherwise indicated. Chemical shifts were reported in parts per million referenced to the residual chloroform proton signal at 7.26 ppm and ^{13}C NMR signal at 77.23 ppm unless otherwise noted. Melting points were taken on a Mel-Temp capillary apparatus and are corrected. Combustion analyses were performed by Desert Analytics, Tucson, AZ and gave results within ±0.4% of theoretical values. All ultraviolet–visible spectra were recorded on a Perkin–Elmer Lambda-12 spectrophotometer. Vapor pressure osmometry (VPO) measurements were performed on an OSMOMAT 070-SA instrument (Gonotech GmbH, Germany) in HPLC grade $CHCl_3$ (Fisher) at 45 °C. Analytical thin layer chromatography (TLC) was carried out on J.T. Baker silica gel IB-F plates (125 μm layer). For final purification, radial chromatography was carried out on Merck silica gel PF_{254} with calcium sulfate binder, preparative layer grade.

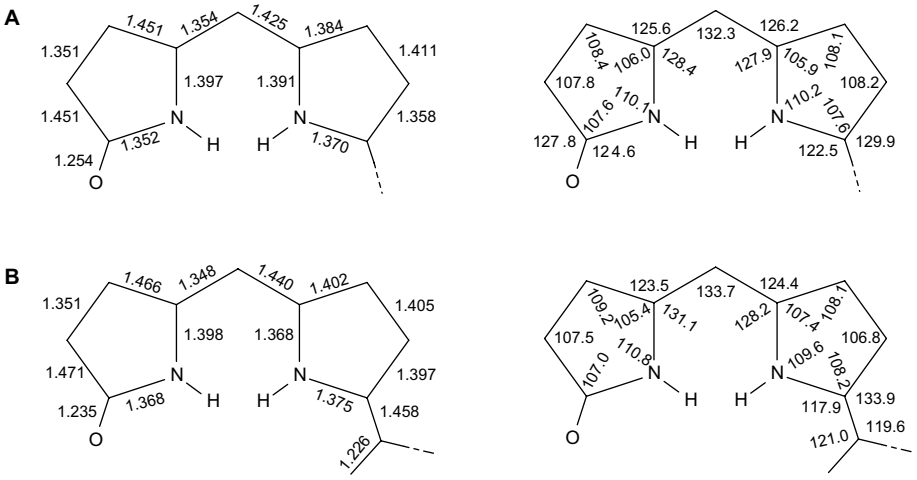

Figure 5. (Left) Bond lengths (Å) and (right) bond angles of (A) tetramethoxy-[6]-semirubin (**1**) and (B) dimethoxy-[6]-oxosemirubin ethyl ester (**4e**) found by X-ray crystallography.

All solvents were of reagent grade obtained from Fisher–Acros. Spectral data were obtained in spectral grade solvents (Aldrich or Fisher). Dipyrrinones **5** and **6** were available from earlier work.[10]

*4.1.1. 9-(5-Carboxypentyl)-2,3,7,8-tetramethoxydipyrrin-1-one (**1**)*

To a solution of oxosemirubin **3** (100 mg, 0.23 mmol) dissolved in 2-propanol, $NaBH_4$ (50 mg, 1.3 mmol) was added and the mixture was heated at reflux for 2.5 h. The reaction mixture was then poured into 80 mL of cold water and acidified carefully to pH 4 to produce a yellow precipitate, which was extracted by CH_2Cl_2, dried, and evaporated in vacuo (rotovap). The crude solid was purified by radial chromatography (95:5 CH_2Cl_2–CH_3OH by vol eluent) to yield 48 mg (50%) of pure **1**. It had mp 92–94 °C; ^{1}H NMR, δ: 1.39 (2H, m), 1.62 (2H, m), 1.70 (2H, m), 2.49 (2H, t, J=7.2 Hz), 2.68 (2H, t, J=7.2 Hz), 3.78 (3H, s), 3.88 (3H, s), 3.90 (s, 3H), 4.11 (s, H), 6.23 (1H, s), 8.38 (1H, br s), 10.11 (1H, br s) ppm; ^{13}C NMR data are in Table 1.

Anal. Calcd for $C_{19}H_{26}N_2O_7$ (394.5): C, 57.86; H, 6.64; N, 7.10. Found: C, 57.97; H, 6.60; N, 7.13.

*4.1.2. 9-(5-Carboethoxypentyl)-2,3,7,8-tetramethoxydipyrrin-1-one (**1e**)*

To a solution of oxosemirubin ester **3e** (300 mg, 0.75 mmol) dissolved in ~10 mL of dry THF at 0 °C (ice–salt bath), ~60 mg $NaBH_4$ was added followed by addition of 3 mL of boron trifluoride etherate ($BF_3\cdot OEt_2O$) in ~8 mL of dry THF over a period of 10 min. The reaction mixture was stirred at 0 °C for 1 h and then quenched by the dropwise addition of methanol. The entire solution was extracted with CH_2Cl_2, and the organic extracts were dried and evaporated in vacuo (rotovap). The crude product was purified using radial chromatography (98:2 CH_2Cl_2–CH_3OH by vol eluent) to afford 183 mg (61%) of **1e**. It had mp 70–71 °C; ^{1}H NMR, δ: 1.24 (3H, t, J=7.5 Hz), 1.37 (2H, m), 1.63 (4H, m), 2.31 (2H, t, J=7.2 Hz), 2.60 (2H, t, J=7.2 Hz), 3.77 (3H, s), 3.91 (3H, s), 4.02 (3H, s), 4.11 (3H, s), 4.12 (2H, q, J=7.5 Hz), 6.00 (1H, s), 8.26 (1H, br s), 9.31 (1H, br s) ppm; ^{13}C NMR data are in Table 1.

Anal. Calcd for $C_{21}H_{30}N_2O_7$ (422.5): C, 59.70; H, 7.16; N, 6.63. Found: C, 59.52; H, 7.10; N, 6.29.

*4.1.3. 9-(5-Carboxypentyl)-2,3-dimethoxy-7,8-dimethyldipyrrin-1-one (**2**)*

To a solution of oxosemirubin **4** (50 mg, 0.12 mmol) dissolved in 2-propanol, $NaBH_4$ (50 mg, 1.3 mmol) was added and the mixture was heated at reflux for 2.5 h. After work-up similar to that for **1** and purification of the crude yellow solid by radial chromatography (95:5 CH_2Cl_2–CH_3OH by vol eluent), 40 mg (92%) of pure **2** was obtained. It had mp 159–161 °C; ^{1}H NMR, δ: 1.39 (2H, m), 1.58 (2H, m), 1.71 (2H, m), 1.93 (3H, s), 2.07 (3H, s), 2.48 (2H, t, J=7.2 Hz), 2.70 (2H, t, J=7.2 Hz), 3.90 (3H, s), 4.13 (3H, s), 6.23 (1H, s), 8.79 (1H, br s), 10.10 (1H, br s) ppm; ^{13}C NMR data are in Table 1.

Anal. Calcd for $C_{19}H_{26}N_2O_5$ (362.5): C, 62.97; H, 7.23; N, 7.73. Found: C, 62.80; H, 6.97; N, 7.73.

*4.1.4. 9-(5-Carboethoxypentyl)-2,3-dimethoxy-7,8-dimethyldipyrrin-1-one (**2e**)*

To a solution of oxosemirubin ester **4e** (200 mg, 0.75 mmol) dissolved in ~10 mL of dry THF at 0 °C (ice–salt bath), ~39 mg of $NaBH_4$ was added, followed by addition of 2 mL of $BF_3\cdot OEt_2O$ in ~8 mL of dry THF over a period of 10 min. The reaction mixture was stirred at room temperature for 1.5 h and then quenched by the dropwise addition of methanol. The product was isolated as per the work-up for **1e** and after radial (98:2 CH_2Cl_2–CH_3OH by vol eluent) chromatography afforded 105 mg (53%) of **2e**. It had mp 139–140 °C; ^{1}H NMR, δ: 1.22 (2H, t, J=7.5 Hz), 1.37 (2H, m), 1.63 (2H, m), 1.65 (2H, m), 1.94 (3H, s), 2.09 (3H, s), 2.26 (2H, t, J=7.2 Hz), 2.73 (2H, t, J=7.2 Hz), 3.85 (3H, s), 4.11 (2H, q, J=7.5 Hz), 4.14 (3H, s), 6.27 (1H, s), 9.70 (1H, br s), 10.45 (1H, br s) ppm; ^{13}C NMR data are in Table 1.

Anal. Calcd for $C_{21}H_{30}N_2O_5$ (390.5): C, 64.60; H, 7.74; N, 7.17. Found: C, 64.96; H, 7.15; N, 6.98.

Table 4
Comparison of the solubility of dipyrrinones (**1**–**4**) in water[a]

Dipyrrinone	[Pigment]f/[pigment]	Solubility at saturation in H_2O (mg/L)
1	(0.85/0.96) 0.89:1.0	24.1
1e	(0.50/1.0) 0.50:1.0	18.5
2	(0.21/0.42) 0.5:1.0	2.4
2e	(0.03/0.81) 0.04:1.0	1.2
3	(0.77/0.80) 0.97:1.0	19.0
3e	(0.75/1.28) 0.59:1.0	14.2
4	(0.70/0.95) 0.74:1.0	13.9
4e	(0.17/0.51) 0.33:1.0	4.3

The ratio of pigment concentration in methanol solvent versus the standard solution (2% $CHCl_3$ in CH_3OH) as compared by UV–vis spectroscopy is 1:1 for all entries.

[a] Ratio of pigment concentration (in H_2O) [pigment]f versus standard solution (2% DMSO in H_2O) [pigment] compared by UV–vis spectroscopy. The standard solutions are prepared and ultrasonicated, the UV–vis absorbance at λ_{max} is recorded. The solution is evaporated to dryness and then the pure solvent (CH_3OH or H_2O) is added, the solution/mixture is ultrasonicated, and the absorbance is remeasured. In all cases it is less than the standard solutions. The ratio of absolute pigment concentrations is found in parentheses, the relative pigment concentrations are outside the parentheses. The methodology is found in the text.

Table 5
Comparison of UV–vis data[a] of semirubins **1** and **2** and their ethyl esters (**1e** and **2e**) and oxosemirubins **3** and **4** and their ethyl esters (**3e** and **4e**)

	$CHCl_3$	CH_3OH	$(CH_3)_2SO$	H_2O
1	407 (32,700)	399 (35,600)	397 (35,300)	398 (33,400)
2	412 (32,500)	404 (35,800)	403 (35,600)	405 (14,500)
3	399 (32,000)	395 (34,200)	393 (33,200)	386 (34,300)
	380 (34,500)	379 (35,000)		
4	414 (31,400)	406 (27,000)	408 (27,900)	391 (27,700)
	395 (31,700)	387 (31,000)	389 (31,100)	
1e	392 (32,700)	398 (36,000)	397 (34,400)	397 (28,000)
2e	400 (33,000)	404 (307,500)	403 (36,500)	405 (11,400)
3e	399 (33,800)	396 (34,200)	390 (36,800)	384 (35,000)
	380 (37,000)	379 (37,500)		
4e	421 (30,000)	417 (29,500)	400 (31,000)	396 (14,600)[b]
	402 (32,300)	400 (32,600)		

[a] Determined for 1×10^{-5} M solutions.
[b] Incompletely soluble.

4.1.5. 9-(5-Carboxypentanoyl)-2,3,7,8-tetramethoxydipyrrin-1-one (**3**)

To a solution of oxosemirubin **3e** (0.23 g, 0.53 mmol) in 100 mL of dry THF and 10 mL of CH_3OH, 0.7 g NaOH was added. The solution was heated at reflux for 2 h under N_2. The reaction mixture was poured into 200 mL of ice-water. The aqueous solution was then acidified with 10% HCl to pH ~4 and then extracted with CH_2Cl_2 until the organic phase became clear. The combined organic phases were dried over anhyd Na_2SO_4 and evaporated in vacuo (rotovap). The crude product was purified by radial chromatography using 3–5% gradient of CH_3OH in CH_2Cl_2. The pure fractions were evaporated in vacuo (rotovap) and recrystallized from CH_2Cl_2–hexane to obtain 183 mg (83%) of **3**. It had mp 190–191 °C; ^{1}H NMR, δ: 1.74 (4H, m), 2.41 (2H, t, J=7.2 Hz), 2.84 (2H, t, J=7.2 Hz), 3.82 (3H, s), 3.95 (3H, s), 4.02 (3H, s), 4.14 (3H, s), 5.96 (1H, s), 8.56 (1H, br s), 9.54 (1H, br s) ppm; ^{13}C NMR data are in Table 1.

Anal. Calcd for $C_{19}H_{24}N_2O_8$ (408.4); C, 55.88; H, 5.92; N, 6.86. Found: C, 55.95; H, 5.60; N, 6.84.

Table 6
Crystal data and structure refinement for **1**

Empirical formula	$C_{19}H_{26}N_2O_7$
Formula weight	391.43
Temperature	100(2) K
Wavelength	0.71073 Å
Crystal system	Monoclinic
Space group	$P2(1)$
Unit cell dimensions	a=8.4287(3) Å, α=90°
	b=24.3892(9) Å, β=98.908(2)°
	c=10.7956(4) Å, γ=90°
Volume	2192.48 (14) Å^3
Z	4
Density (calculated)	1.489 mg m^{-3}
Absorption coefficient	0.339 mm^{-1}
F(000)	1064
Crystal size	0.51×0.13×0.09 mm^3
θ Range for data collection	1.67–25.00°
Index ranges	$-10\le h\le 9$, $-28\le k\le 28$, $-12\le 1\le 12$
Reflections collected	28,076
Independent reflections	7646 [R(int)=0.0647]
Completeness to θ=25.00°	100.0%
Absorption correction	SADABS
Max and min transmission	0.9717 and 0.8460
Refinement method	Full-matrix least-squares on F^2
Data/restraints/parameters	7646/1/552
Goodness-of-fit on F^2	1.049
Final R indices [$I>2\sigma(I)$]	$R1$=0.0514, $wR2$=0.1270
R Indices (all data)	$R1$=0.0704, $wR2$=0.1359
Absolute structure parameter	0.65(8)
Extinction coefficient	0.0000(6)
Largest diff. peak and hole	0.651 and −0.335 e Å^{-3}

Table 7
Crystal data and structure refinement for **4e**

Empirical formula	$C_{21}H_{28}N_2O_6$
Formula weight	404.46
Temperature	100(2) K
Wavelength	0.71073 Å
Crystal system	Monoclinic
Space group	$P2(1)/n$
Unit cell dimensions	a=11.9799(2) Å, α=90°
	b=6.65120(10) Å, β=97.2290(10)°
	c=25.8469(5) Å, γ=90°
Volume	2043.13(6) Å^3
Z	4
Density (calculated)	1.354 mg m^{-3}
Absorption coefficient	0.098 mm^{-1}
F(000)	912
Crystal size	0.36×0.14×0.06 mm^3
θ Range for data collection	1.59–25.00°
Index ranges	$-14\le h\le 14$, $-7\le k\le 7$, $-30\le 1\le 30$
Reflections collected	17,443
Independent reflections	3591 [R(int)=0.0294]
Completeness to θ=25.00°	100.0%
Absorption correction	SADABS
Max and min transmission	0.9941 and 0.9656
Refinement method	Full-matrix least-squares on F^2
Data/restraints/parameters	3591/0/268
Goodness-of-fit on F^2	1.015
Final R indices [$I>2\sigma$ (I)]	$R1$=0.0348, $wR2$=0.0826
R Indices (all data)	$R1$=0.0397, $wR2$=0.0850
Extinction coefficient	0.0067(8)
Largest diff. peak and hole	0.242 and −0.227 e Å^{-3}

4.1.6. 9-(5-Carboethoxypentanoyl)-2,3,7,8-tetramethoxydipyrrin-1-one (**3e**)

To a cooled mixture of half ethyl ester acid chloride of adipic acid (0.3 g, 1.57 mmol) and $SnCl_4$ (1.03 g, 3.93 mmol) in 50 mL CH_2Cl_2, a solution of 9*H*-tetramethoxydipyrrinone **5** (110 mg, 0.39 mmol) in 50 mL of CH_2Cl_2 was added dropwise. The solution was stirred at room temperature for 7 h with constant checking by TLC. The reaction mixture was poured into 100 g ice-water and stirred for 2 h. The organic layer was separated and aqueous layer was washed with CH_2Cl_2 (2×100 mL). The combined organic layers were washed with 5% aq $NaHCO_3$ and then with water, dried over anhyd Na_2SO_4, and evaporated in vacuo (rotovap). The crude product was purified by flash column chromatography (98:2 CH_2Cl_2–CH_3OH by vol eluent) followed by radial chromatography (98:2 CH_2Cl_2–CH_3OH by vol eluent) to obtain pure **3e** in 47% yield. It had mp 98–100 °C ^{1}H NMR, δ: 1.74 (4H, m), 2.34 (2H, t, J=7.2 Hz), 2.84 (2H, t, J=7.2 Hz), 3.83 (3H, s), 3.95 (3H, s), 4.02 (3H, s), 4.10 (3H, s), 5.99 (1H, s), 8.50 (1H, br s), 9.55 (1H, br s) ppm; ^{13}C NMR data are in Table 1.

Anal. Calcd for $C_{21}H_{28}N_2O_8$ (436.5): C, 57.79; H, 6.47; N, 6.42. Found: C, 57.69; H, 6.39; N, 6.40.

4.1.7. 9-(5-Carboxypentanoyl)-2,3-dimethoxy-7,8-dimethyldipyrrin-1-one (**4**)

To a solution of oxosemirubin **4e** (0.25 g, 0.62 mmol) in 100 mL of dry THF and 10 mL of CH_3OH was added 0.7 g NaOH, and the mixture was heated at reflux for 2 h under N_2. The reaction mixture was treated as in the synthesis of **3** and worked up in the same way to give pure fractions, which were evaporated in vacuo (rotovap) and recrystallized from CH_2Cl_2–hexane to obtain 201 mg (87%) of **4**. It had mp 162–163 °C; ^{1}H NMR, δ: 1.82 (2H, m), 1.85 (2H, m), 2.04 (3H, s), 2.29 (3H, s), 2.46 (2H, t, J=7.2 Hz), 2.82 (2H, t, J=7.2 Hz), 3.92 (3H, s), 4.14 (3H, s), 6.16 (1H, s), 9.25 (1H, br s), 9.97 (1H, br s) ppm; ^{13}C NMR data are in Table 1.

Anal. Calcd for $C_{19}H_{24}N_2O_6\cdot1/2H_2O$ (385.4): C, 59.21; H, 6.54; N, 7.27. Found: C, 59.88; H, 6.36; N, 7.03.

*4.1.8. 9-(5-Carboethoxypentanoyl)-2,3-dimethoxy-7,8-dimethyldipyrrin-1-one (**4e**)*

To a cooled mixture of half ethyl ester acid chloride of adipic acid (0.12 g, 0.65 mmol) and $SnCl_4$ (0.29 g, 1.13 mmol) in 50 mL of CH_2Cl_2, a solution of 9*H*-dimethoxydipyrrinone **6** (40 mg, 0.16 mmol) in 50 mL of CH_2Cl_2 was added dropwise. The solution was stirred at room temperature for 12 h and then poured into 100 g of ice-water and stirred for 2 h. The organic layer was separated and the aqueous layer was washed with CH_2Cl_2 (2×100 mL). The combined organic layers were washed with aq $NaHCO_3$ and then with water, dried over anhyd Na_2SO_4, and evaporated in vacuo (rotovap). The crude product was purified by flash column (95:5 CH_2Cl_2–CH_3OH by vol eluent) and then by radial (98:2 CH_2Cl_2–CH_3OH by vol eluent) chromatography to obtain pure **4e** in 60% yield. It had mp 158–159 °C; ^{1}H NMR, δ: 1.25 (3H, t, J=7.4 Hz), 1.75 (4H, m), 2.05 (3H, s), 2.28 (3H, s), 2.36 (2H, t, J=7.2 Hz), 2.79 (2H, t, J=7.2 Hz), 4.02 (3H, s), 4.11 (2H, q, J=7.4 Hz), 4.33 (3H, s), 6.07 (1H, s), 7.62 (1H, br s), 10.76 (1H, br s) ppm; ^{13}C NMR data are in Table 1.

Anal. Calcd for $C_{21}H_{28}N_2O_6$ (404.5): C, 62.36; H, 6.98; N, 6.93. Found: C, 62.29; H, 6.70; N, 6.85.

4.2. X-ray structures

Crystals of **1** were grown by slow diffusion of diethyl ether into a solution of CH_2Cl_2. Crystals of **4e** were grown by slow diffusion of diethyl ether into a solution of $CHCl_3$. A crystal of **1** (0.51×0.13×0.09 mm^3) and a crystal of **4e** (0.36×0.14×0.06 mm^3) were placed onto the tips of 0.1 mm diameter glass capillaries and mounted on a Bruker SMART Apex system for data collection at 100(2) K. A preliminary set of cell constants was calculated from reflections harvested from three sets of 20 frames for **1** and **4e**. These initial sets of frames were oriented such that orthogonal wedges of reciprocal space were surveyed (final orientation matrices determined from global least-squares refinement of 7646 reflections for **1** and 3591 reflections for **4e**). The data collection was carried out using Mo Kα radiation (0.71073 Å graphite monochromator) with a frame time of 40 s for **1** and 30 s for **4e** and a detector distance of 4.94 cm. A randomly oriented region of reciprocal space was surveyed to the extent of two hemispheres and to a resolution of 0.66 Å. Four major sections of frames were collected with 0.3° steps in ω at 600 different φ settings and a detector position of 36° in 2θ for **1** and **4e**. The intensity data were corrected for absorption and decay (SADABS).[13] Final cell constants were calculated from the *xyz* centroids of strong reflections from the actual data collection after integration (SAINT 6.45, 2003).[14] Crystal data and refinement information for **1** and **4e** are provided in Tables 6 and 7, respectively.

The structures were solved and refined using SHELXLT-L.[15] The monoclinic space groups *P*2(1) and *P*2(1)/*n* were determined for **1** and **4e**, respectively, based on systematic absences and intensity statistics. A direct-methods solution was calculated, which provided non-hydrogen atoms from the *E*-map. Full-matrix least-squares/difference Fourier cycles were performed for structure refinement. All non-hydrogen atoms were refined with anisotropic displacement parameters unless stated otherwise. Hydrogen atom positions were placed in ideal positions and refined as riding atoms with relative isotropic displacement parameters (a C–H distance fixed at 0.96 Å and a thermal parameter 1.2 times the host carbon atom). Tables of atomic coordinates, bond lengths and angles, anisotropic displacement parameters, hydrogen coordinates, and isotropic displacement parameters have been deposited at the Cambridge Crystallographic Data Centre, CCDC No. 703014 for **1** and 703013 for **4e**.

Acknowledgements

We thank the U.S. National Institutes of Health (HD 17779) for generous support of this research. We also thank the National Science Foundation (CHE-0226402 and CHE-0521191) for providing funding to purchase the X-ray diffractometer used in this work and acquiring a 400 MHz NMR spectrometer and upgrading an existing unit. We thank Prof. T.W. Bell for use of the vapor pressure osmometer.

References and notes

1. (a) Chowdhury, J. R.; Wolkoff, A. W.; Chowdhury, N. R.; Arias, I. M. In *The Metabolic and Molecular Bases of Inherited Disease*; Scriver, C. F., Beaudet, A. L., Sly, W. S., Valle, D., Eds.; McGraw-Hill: New York, NY, 2001; Chapter 125, pp 3063–3101; (b) McDonagh, A. F. In *The Porphyrins*, Vol. VI (Dolphin, D., Ed.) Academic: New York, NY, Chapter 6, pp 1979.
2. Brodersen, R. In *Bilirubin*; Heirwegh, K. P. M., Brown, S. B., Eds.; CRC: Boca Raton, FL, 1986; Vol. I, Chapter 3, p 76.
3. (a) Bonnett, R.; Davies, J. E.; Hursthouse, N. B.; Sheldrick, G. M. *Proc. R. Soc. London, Ser. B* **1978**, *202*, 249–268; (b) LeBas, G.; Allegret, A.; Mauguen, Y.; DeRango, C.; Bailly, M. *Acta Crystallogr., Sect. B* **1980**, *B36*, 3007–3011; (c) Becker, W.; Sheldrick, W. S. *Acta Crystallogr., Sect. B* **1978**, *B34*, 1298–1304.
4. Person, R. V.; Peterson, B. R.; Lightner, D. A. *J. Am. Chem. Soc.* **1994**, *116*, 42–49.
5. Falk, H. *The Chemistry of Linear Oligopyrroles and Bile Pigments*; Springer: Wien, 1989.
6. Boiadjiev, S. E.; Lightner, D. A. *Org. Prep. Proced. Int.* **2006**, *38*, 347–399.
7. Huggins, M. T.; Lightner, D. A. *J. Org. Chem.* **2000**, *65*, 6001–6008.
8. Boiadjiev, S. E.; Watters, K.; Lai, B.; Wolf, S.; Welch, W.; McDonagh, A. F.; Lightner, D. A. *Biochemistry* **2004**, *43*, 15617–15632.
9. (a) Merz, A.; Schroppe, R.; Dötterl, E. *Synthesis* **1995**, 795–800; (b) Wie, W.-H.; Wang, A.; Mizuno, T.; Cortez, C.; Fu, L.; Siriwasad, M.; Naumorski, L.; Magda, D.; Sessler, J. L. *Dalton Trans.* **2006**, 1934–1942; (c) Schmuck, C.; Wienand, W. *J. Am. Chem. Soc.* **2003**, *125*, 452–459.
10. (a) Dey, S. K.; Lightner, D. A. *Monatsh. Chem.* **2007**, *138*, 687–697;(b) Dey, S.K.; Lightner, D.A. *Monatsh. Chem.*, in press.
11. Huggins, M. T.; Lightner, D. A. *Monatsh. Chem.* **2001**, *132*, 203–221.
12. (a) Cullen, D. L.; Pèpe, G.; Meyer, E. F., Jr.; Falk, H.; Grubmayr, K. *J. Chem. Soc., Perkin Trans. 2* **1979**, 999–1004; (b) Cullen, D. L.; Black, P. S.; Meyer, E. F., Jr.; Lightner, D. A.; Quistad, G. B.; Pak, C. S. *Tetrahedron* **1977**, *33*, 477–483.
13. Sheldrick, G. M. *SADABS, vers. 2.1*; Bruker Analytical X-ray Systems: Madison, WI, 2003.
14. *SAINT, vers. 6.45*; Bruker Analytical X-ray Systems: Madison, WI, 2003.
15. Sheldrick, G. M. *SHELXT-L, vers. 6.14*; Bruker Analytical X-ray Systems: Madison, WI, 1997.